Article

SOURCE DATA | TRANSPARENT PROCESS

THE EMBO JOURNAL

OPA1-dependent cristae modulation is essential for cellular adaptation to metabolic demand

David A Patten[1], Jacob Wong[1], Mireille Khacho[1], Vincent Soubannier[2], Ryan J Mailloux[3], Karine Pilon-Larose[1], Jason G MacLaurin[1], David S Park[1], Heidi M McBride[2], Laura Trinkle-Mulcahy[1], Mary-Ellen Harper[3], Marc Germain[4,**] & Ruth S Slack[1,*]

Abstract

Cristae, the organized invaginations of the mitochondrial inner membrane, respond structurally to the energetic demands of the cell. The mechanism by which these dynamic changes are regulated and the consequences thereof are largely unknown. Optic atrophy 1 (OPA1) is the mitochondrial GTPase responsible for inner membrane fusion and maintenance of cristae structure. Here, we report that OPA1 responds dynamically to changes in energetic conditions to regulate cristae structure. This cristae regulation is independent of OPA1's role in mitochondrial fusion, since an OPA1 mutant that can still oligomerize but has no fusion activity was able to maintain cristae structure. Importantly, OPA1 was required for resistance to starvation-induced cell death, for mitochondrial respiration, for growth in galactose media and for maintenance of ATP synthase assembly, independently of its fusion activity. We identified mitochondrial solute carriers (SLC25A) as OPA1 interactors and show that their pharmacological and genetic blockade inhibited OPA1 oligomerization and function. Thus, we propose a novel way in which OPA1 senses energy substrate availability, which modulates its function in the regulation of mitochondrial architecture in a SLC25A protein-dependent manner.

Keywords ATP synthase; cristae; mitochondria; OPA1; SLC25A
Subject Categories Membrane & Intracellular Transport; Metabolism
DOI 10.15252/embj.201488349 | Received 27 February 2014 | Revised 28 August 2014 | Accepted 29 August 2014 | Published online 8 October 2014
The EMBO Journal (2014) 33: 2676–2691

Introduction

Mitochondria are vital to a number of important cell functions including energy production through oxidative phosphorylation (OXPHOS), calcium buffering and apoptotic signalling. These dynamic organelles constantly modify their architecture and undergo fission and fusion. Mitochondrial fusion is mediated by the two outer membrane mitofusins (MFN1 and MFN2) (Chen *et al*, 2003) and the inner membrane optic atrophy 1 (OPA1) (Meeusen *et al*, 2006). Mitochondrial fusion and fission are important processes for cell survival during a variety of stressors (Tondera *et al*, 2009; Gomes *et al*, 2011) and are dysregulated or disrupted in a number of human pathologies (Alexander *et al*, 2000; Delettre *et al*, 2000; Zuchner *et al*, 2004). Mitochondria also undergo internal cristae changes. Cristae, being invaginations of the inner membrane, form internal compartments which are connected to the inner boundary membrane (IBM) by tight cristae junctions. Cristae possess different proteins than the IBM arguing that they are functionally distinct compartments (Vogel *et al*, 2006; Wurm & Jakobs, 2006). Tight cristae, and their junctions, may restrict diffusion of small molecules and membrane proteins into and out of cristae (Mannella, 2006b; Sukhorukov & Bereiter-Hahn, 2009).

Changes in inner membrane topology have been documented during apoptosis, as cristae junction widening is required to mobilize cytochrome *c* stores for release upon outer membrane permeabilization (Scorrano *et al*, 2002; Germain *et al*, 2005; Frezza *et al*, 2006). Cristae structural changes during non-cell death stimuli have also been reported for many decades, but their regulation and function remain elusive. For example, isolated liver mitochondria display different reversible ultrastructure conformations according to their energetic state (Hackenbrock, 1966). Hackenbrock named these two states *orthodox* and *condensed*, where condensed mitochondria have a compacted matrix with enlarged cristae and orthodox mitochondria have a less dense matrix with compacted cristae. Similarly, starvation increases mitochondrial length and the number of cristae (Gomes *et al*, 2011), suggesting that mitochondria regulate their shape to adjust their activity with metabolic conditions (Mannella, 2006a). Furthermore, it was recently shown that cristae shape regulates respiration through the assembly of respiratory chain supercomplexes (Cogliati *et al*, 2013).

In addition to fusion, OPA1 and Mgm1, the yeast homologue of OPA1, are required for cristae structure as their disruption

1 Department of Cellular & Molecular Medicine, University of Ottawa, Ottawa, ON, Canada
2 Montreal Neurological Institute, McGill University, Montreal, QC, Canada
3 Department of Biochemistry, Microbiology & Immunology, University of Ottawa, Ottawa, ON, Canada
4 Département de Biologie Médicale, Université du Québec à Trois-Rivières, Trois-Rivières, QC, Canada
*Corresponding author. Tel: +1 613 562 5800; E-mail: rslack@uottawa.ca
**Corresponding author. Tel: +1 819 376 5011 x3330; E-mail: marc.germain1@uqtr.ca

drastically affects cristae morphology (Amutha *et al*, 2004; Frezza *et al*, 2006; Meeusen *et al*, 2006). Maintenance of cristae structure by OPA1 requires its oligomerization since during apoptosis, disruption of OPA1 oligomers is necessary for cristae opening and cytochrome *c* mobilization (Frezza *et al*, 2006). In fact, cytochrome *c* release and apoptosis could be inhibited by expressing mutant OPA1(Q297V), which mimics OPA1's GTP-bound state and remains self-assembled (Yamaguchi *et al*, 2008). However, the impact of physiological metabolic changes on OPA1 assembly, cristae and mitochondrial respiration is unknown.

Here, we demonstrate that OPA1 dynamically regulates cristae shape in healthy cells and that this process is required to maintain mitochondrial activity under conditions of low-energy substrate availability. Specifically, lack of energy substrates induced OPA1 oligomerization and narrowing of cristae, which was required to promote ATP synthase assembly and to maintain ATP-linked respiration. Importantly, these changes were independent of mitochondrial fusion and essential for cell survival. We also identified a group of mitochondrial solute carriers that interact with OPA1 to regulate its function. Taken together, our results demonstrate that OPA1-dependent modulation of cristae structure is necessary for cellular adaptation to energy substrate availability and is required for cell growth and survival.

Results

OPA1 responds rapidly and reversibly to metabolic demand

Although mitochondrial structural changes in response to energetic states have been documented for decades, their regulation and functional significance have remained largely unknown. To ask whether cristae structure responds to changes in nutrient conditions, mouse embryonic fibroblasts (MEFs) were starved with EBSS for 2 h and cristae were measured. We observed a significant thinning of cristae width and mitochondrial width in response to starvation (Fig 1A). While untreated cells had an average cristae width of 17.6 nm, starved cells had an average width of only 11.9 nm. Since the deoligomerization of OPA1 regulates cristae widening during cell death signalling (Frezza *et al*, 2006), we assessed the oligomerization status of OPA1 in response to starvation. Starved MEFs exhibited significantly more oligomerized OPA1 than fed controls (Fig 1B and D). At longer time points, we also observed that mitochondria elongate from an average length of 3.3 to 4.2 μm, $P = 0.022$ (distribution in Fig 1C). This previously documented elongation has been substantiated by a decrease in mitochondrial fission through DRP-1 inhibition leading to unopposed mitochondrial fusion (Gomes *et al*, 2011; Rambold *et al*, 2011). Unlike elongation, the oligomerization of OPA1 in response to starvation was rapid (within 1 h) and preceded activation of the autophagic pathway as indicated by p62 degradation (Fig 1D). Furthermore, changes in OPA1 oligomerization were rapidly reversible, since incubation of starved MEFs for only 30 min in recovery media (regular growth media) reversed the increase in oligomerized OPA1 (Fig 1E). Together, these data suggest that changes in OPA1 oligomers are linked to changes in cristae structure not only during cell death as previously demonstrated (Frezza *et al*, 2006), but also in healthy cells following changes in energy substrate availability.

To assess how OPA1 responds to changes in fuel substrate availability, we turned to an *in vitro* system. Isolated mitochondria were incubated in the absence or the presence of ETC substrates and crosslinked. When mitochondria were fed with complex I and II substrates (malate plus glutamate or succinate, respectively), OPA1 oligomerization was dramatically reduced compared to no substrate, starved controls [Fig 2A (EDC crosslinking) and Supplementary Fig S1A (BMH crosslinking)]. As we would predict, the same concentration of glucose, the principal glycolysis substrate, had no effect on OPA1 oligomerization (Fig 2A). As in starved cells, OPA1 oligomerization was rapidly reversible upon the addition or removal of complex I substrates (Fig 2B). Next, we asked whether changes in OPA1 oligomerization correlated with altered mitochondrial structure. This was assessed by mitochondrial inter-cristae cytochrome *c* retention, as a readout of cristae structure, since an increase in releasable cytochrome *c* following outer membrane solubilization correlates with wider cristae (Scorrano *et al*, 2002; Wasilewski *et al*, 2012). Following the addition of a low concentration of digitonin to specifically solubilize the outer membrane [1 μg/μg mitochondria, at 0.1% w/v—experimentally determined (Supplementary Fig S1B)], significantly more cytochrome *c* was mobilized when mitochondria were incubated in the presence of complex I and II substrates, compared to the absence of substrates (Fig 2C). Furthermore, this increase in cytochrome *c* mobilization, indicative of cristae widening, was reversible (Supplementary Fig S1C), correlating with the decrease in OPA1 oligomerization and a decrease in orthodox mitochondria, which demonstrates tighter cristae morphology (Supplementary Fig S1D and E). The regulation of cytochrome *c* retention was OPA1 dependent, since mitochondria from OPA1 KO cells had very high levels of mobilized cytochrome *c* independently of the presence of complex I substrates (Fig 2D). We next asked whether the substrate-dependent changes in OPA1 oligomerization were secondary to changes in electron transport chain (ETC) activity. To this end, we added rotenone, a complex I poison, and CCCP, a mitochondrial uncoupler, to the mitochondrial preparations. Neither rotenone nor CCCP altered OPA1 oligomerization (Fig 2E and F), suggesting that OPA1 responds to energy substrate availability upstream of changes in mitochondrial respiration and ETC function.

These studies reveal a strict correlation between energy substrate level, cristae structure and OPA1 oligomerization in which mitochondria enriched with substrates show low levels of OPA1 oligomers and mobilized cytochrome *c* from cristae stores, and starved mitochondria show high levels of OPA1 oligomers and tight cristae. We next sought out the physiological relevance of this cristae regulation as well as the mechanism by which OPA1 senses energy substrate availability.

OPA1 is required for regulation of cristae structure and cell survival during starvation

To address the physiological importance of OPA1-dependent cristae remodelling in response to changes in energy substrate conditions, we first asked whether OPA1 KO cells, devoid of cristae, could survive cellular starvation. While WT MEFs were minimally affected by 6 h of EBSS starvation, OPA1 KO MEFs showed a dramatic increase in cell death, as recently published (Fig 3A, Supplementary Fig S2A and B) (Gomes *et al*, 2011). As survival of starved cells has

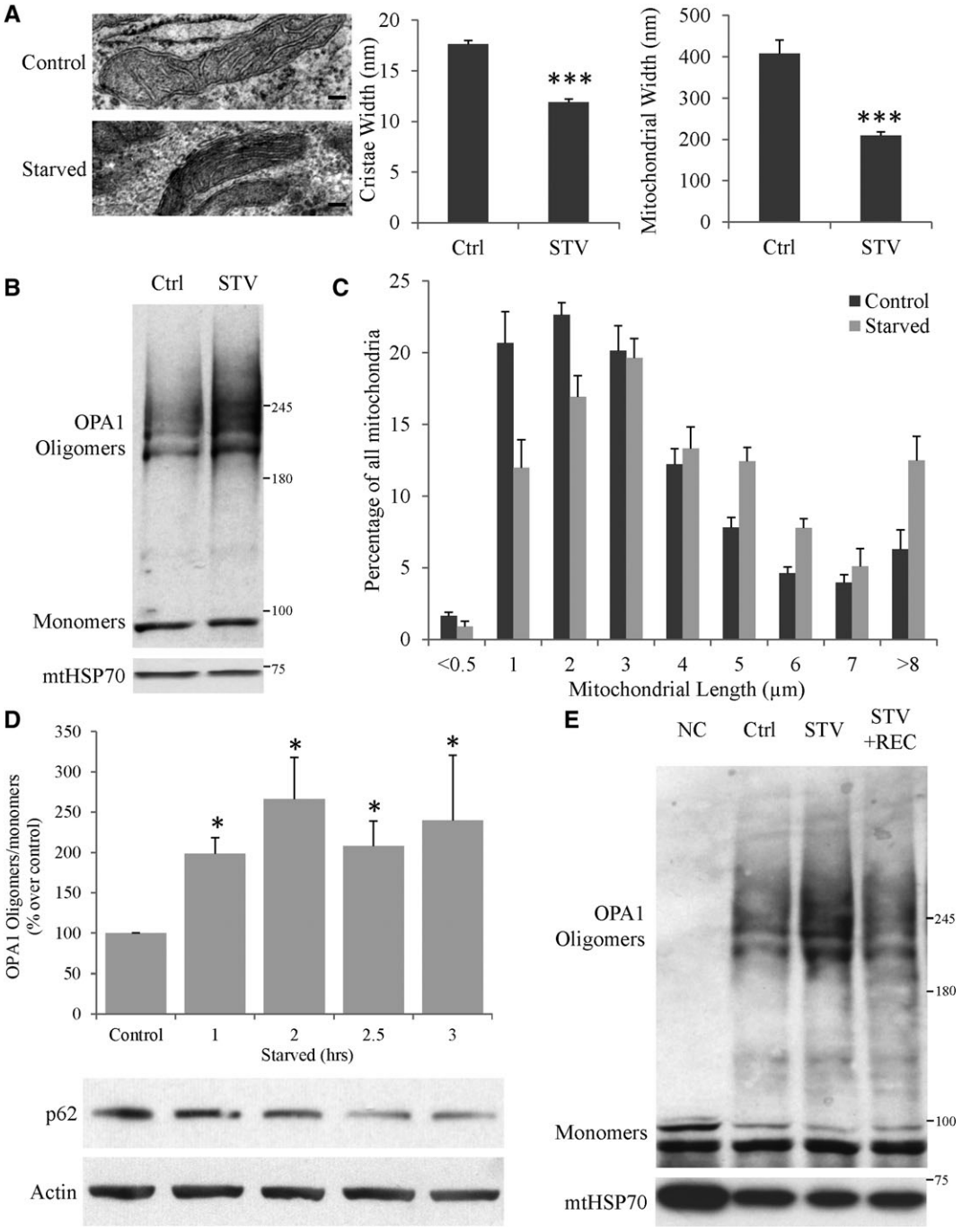

Figure 1. Cristae condense, mitochondria elongate and OPA1 oligomerizes rapidly and reversibly during cell starvation.

A MEFs were starved (STV) or not (Ctrl) for 2 h, fixed with 2% PFA and 1.6% glutaraldehyde and analysed by EM. Cristae and mitochondrial width were quantified from mitochondria and cristae within 10 cells from two independent cultures (n = 20). Scale bars: 100 nm.

B Cells were starved or not for 2 h and crosslinked with BMH (1 mM), and OPA1 oligomerization was analysed by gradient gel Western blot.

C MEFs were starved for 4 h and fixed, and mitochondrial length was measured by immunofluorescence using Tom20 antibodies (averages ± SEM of three independent experiments).

D Time-course experiment of EBSS starvation on OPA1 oligomerization status as performed in (B) (averages ± SEM of four independent experiments). Whole-cell lysates of a parallel experiment were analysed by Western blot.

E After 2 h of EBSS starvation, MEFs were recovered (REC) in regular growth media for 30 min or not and OPA1 oligomers were then analysed as above. A non-crosslinked control (NC) is also included.

Data information: Student's t-tests were performed relative to control, $^*P < 0.05$, $^{***}P < 0.005$.
Source data are available online for this figure.

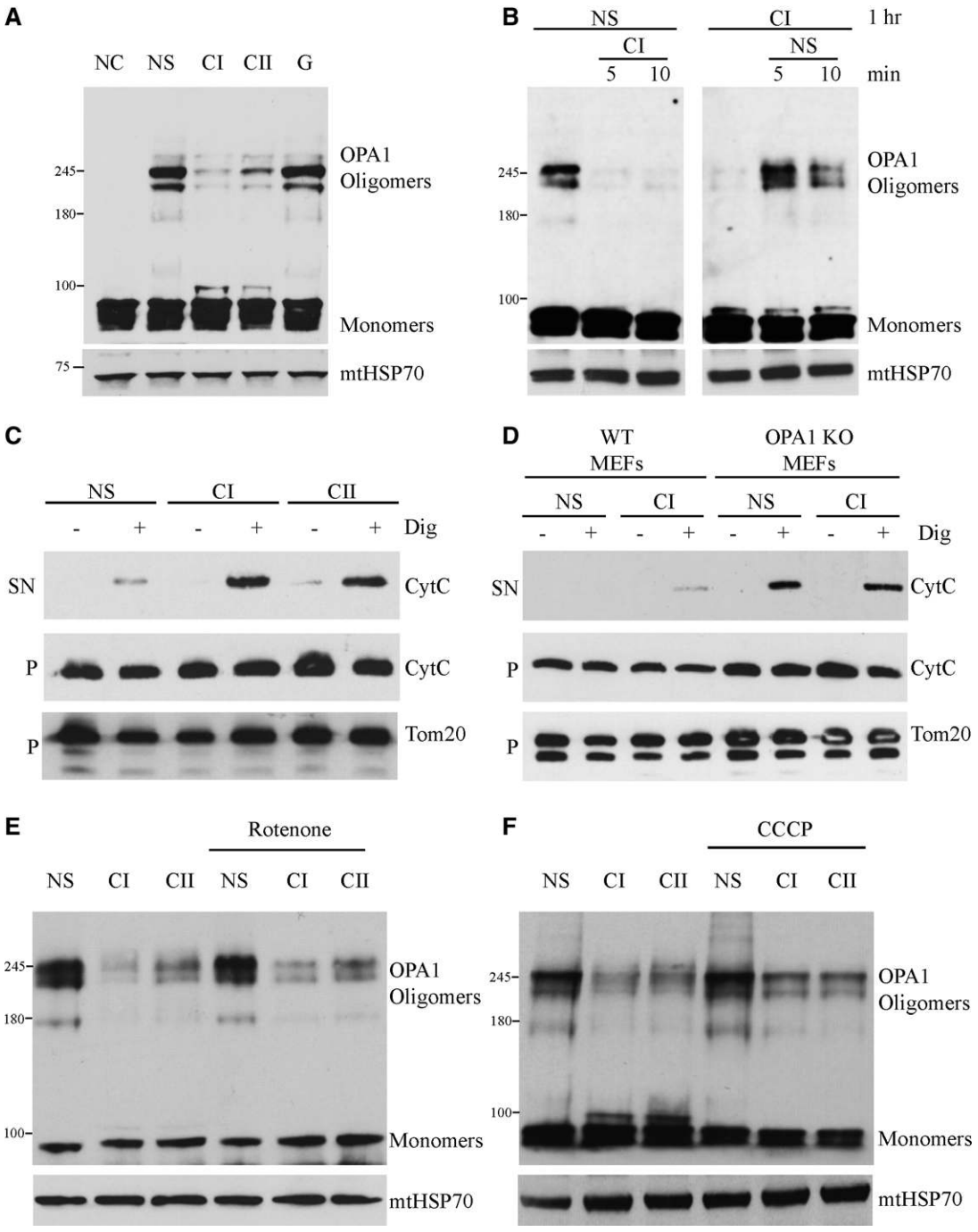

Figure 2. OPA1 responds to energy substrate availability and responds by oligomerizing and maintaining cytochrome *c* in isolated mitochondria.

A OPA1 oligomerization was analysed in isolated mouse liver mitochondria incubated with or without the indicated ETC substrates (NC: non-crosslinked control; NS: no substrate control; CI: complex I, malate and glutamate; CII: complex II, succinate; G: glucose control; all at 5 mM each) for 1 h at 37°C and subsequently crosslinked with EDC for 30 min at room temperature. OPA1 oligomers were then analysed by gradient gel Western blot.

B Mitochondria were incubated with or without complex I substrates, spun down and resuspended in the indicated buffer for 5 and 10 min and analysed as above.

C Mitochondrial ultrastructure was analysed as the distribution of intercristal cytochrome *c* from liver mitochondria and solubilized with low digitonin concentrations (1 μg/μg mitochondria, 0.1%). Mobilized cytochrome *c* was separated by centrifugation and visualized by Western blot analysis where released cytochrome *c* was redistributed from the pellet (P) to the supernatant (SN) fraction.

D Cytochrome *c* mobilization was analysed on mitochondria isolated from WT and OPA1 KO MEFs treated as indicated.

E Liver mitochondria were incubated with or without indicated substrates as above with or without rotenone (2 μM), an ETC complex I poison.

F Liver mitochondria were incubated with or without indicated substrates as above with or without CCCP (10 μM), a mitochondrial uncoupler.

Source data are available online for this figure.

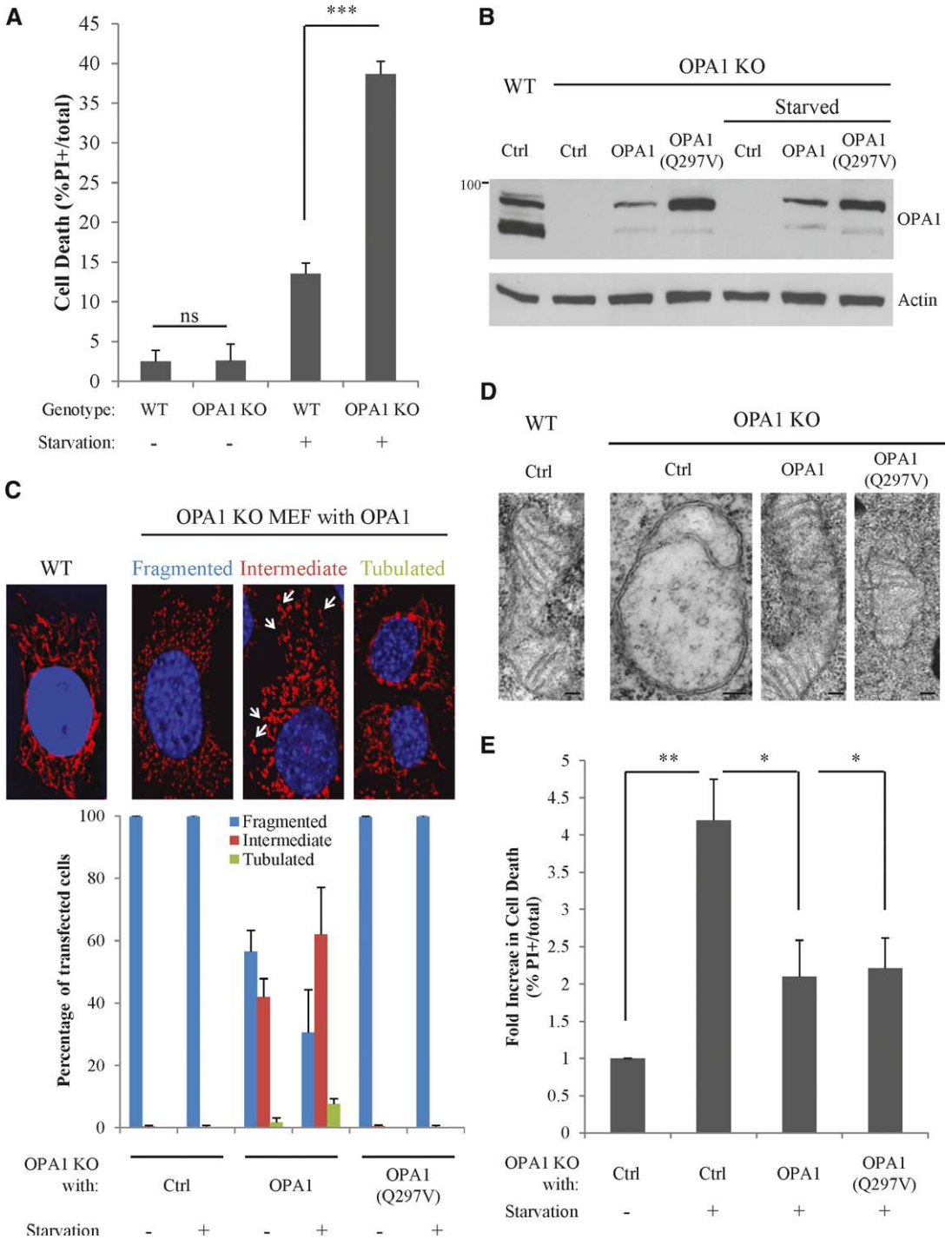

Figure 3. OPA1 is required for resistance to starvation-induced cell death independently of its fusion activity.

A Cell death of WT and OPA1 KO cells starved or not for 6 h was analysed with propidium iodide (PI) and Hoechst (averages ± SEM of four independent experiments).

B Representative Western blot of OPA1 expression in the transient transfection experiments performed in (C–E).

C OPA1 KO MEFs were transiently transfected for 48 h with the indicated plasmids, and mitochondrial length was binned according to the top panels by immunofluorescence where cells that had any long mitochondria were binned as intermediate (averages ± SEM of three independent experiments).

D Representative EM of mitochondria from cells transfected as indicated. Scale bars: 100 nm.

E OPA1 KO MEFs were transfected as indicated for 48 h and starved or not for 6 h, and cell death was analysed as in (A) (averages ± SEM of four independent experiments).

Data information: Student's *t*-tests were performed as indicated, $*P < 0.05$, $**P < 0.01$ and $***P < 0.005$.
Source data are available online for this figure.

been suggested to require mitochondrial elongation through unopposed fusion (Gomes *et al*, 2011), we isolated the roles of fusion and cristae structure using a mutant form of OPA1 that fails to mediate fusion. OPA1(Q297V) mimics the GTP-bound state of OPA1, allowing oligomerization, but defective in GTPase activity, which is required to mediate fusion (Misaka *et al*, 2002; Yamaguchi *et al*, 2008). To assess their ability to rescue mitochondrial fusion and cristae structure, isoform 1 of WT OPA1 or isoform 1 of OPA1(Q297V) was reintroduced in OPA1 KO MEFs by transient transfections, resulting in the expression of mostly the long form with some cleaved short form (Fig 3B). While WT OPA1 rescued fusion, the OPA1(Q297V) mutant was completely fusion incompetent, despite that it was expressed at slightly higher levels than WT OPA1 (Fig 3B and C). To assess whether OPA1 (Q297V) can rescue the cristae structural defects seen in OPA1 KO cells, we performed transmission electron microscopy (EM). Both WT and OPA1(Q297V) rescued the severe cristae defects found in OPA1 KO MEFs (Fig 3D) and rescued survival of OPA1 KO MEFs during starvation (Fig 3E, Supplementary Fig S2C). These results suggest that OPA1 protects against starvation-induced cell death independently of its fusion activity.

OPA1 maintains mitochondrial function independently of its fusion activity

The rescue of cristae structure and cell survival by OPA1 and a fusion-incompetent mutant suggests that cristae modulation is a key determinant of cellular survival under changing energetic demands. To assess whether OPA1-mediated cristae alterations alone can affect cellular metabolism, we generated MEFs stably expressing OPA1 or OPA1(Q297V), resulting in high expression of both the long and short isoforms of OPA1 (Fig 4A). As in the transient system, OPA1(Q297V) rescued cristae structure in OPA1-deficient MEFs but not mitochondrial fusion (Supplementary Fig S3A and B). In addition, both WT and OPA1(Q297V) oligomerized and responded to substrate-level changes in isolated mitochondria from stable cell lines (Fig 4B).

To address how OPA1-mediated control of cristae modulates mitochondrial energetics, we assessed cellular oxygen consumption characteristics after OPA1 reintroduction using the Seahorse XF-24 analyzer (Fig 4C–E). Under fuel-rich conditions, a modest difference in ATP-linked respiration (the difference between the initial resting respiration and the respiration in the presence of oligomycin, a complex V inhibitor) was observed between WT and OPA1 KO MEFs (Fig 4C, Supplementary Fig S4A and B). However, starvation increased the difference in ATP-linked oxygen consumption between WT and OPA1 KO cells (Fig 4D, Supplementary Fig S4A and B), consistent with a requirement for OPA1 to maintain mitochondrial ATP levels under starvation (Gomes *et al*, 2011). We next addressed whether OPA1(Q297V) rescued oxygen consumption. Under resting (fed) conditions, only expression of the WT form of OPA1 significantly increased ATP-linked respiration of OPA1 KO MEFs (Fig 4C and quantified in E). However, after starvation, both the WT and OPA1(Q297V) significantly increased ATP-linked oxygen consumption (Fig 4D and E). Only WT OPA1 reintroduction completely rescued maximal respiration (oligomycin and FCCP, a mitochondrial uncoupler) and thus the reserve capacity (the difference between the resting and maximal respiration) (Fig 4E). These functional studies demonstrate that the critical role of OPA1 in regulating mitochondrial metabolism is fusion independent; however, mitochondrial fusion is required for full maximal oxygen consumption, possibly through maintenance of mtDNA (see below), which may be important following other various stressors.

To further investigate the role of cristae and mitochondrial fusion in mitochondrial function, cells were grown in a galactose medium in which they must rely on OXPHOS for ATP production (Aguer *et al*, 2011; Cogliati *et al*, 2013). While WT and OPA1 KO MEFs grew at similar rates in glucose media, OPA1 KO cells were growth retarded in galactose media compared to WT MEFs (Fig 4F). In fact, in the third week of growth in galactose media, it took more than twice as long for OPA1 KO cells to double their numbers (Supplementary Fig S5). Reintroducing WT or OPA1(Q297V) rescued growth retardation in OPA1 KO MEFs (Fig 4F, Supplementary Fig S5), providing further evidence that OPA1 can maintain mitochondrial function to support cell growth, independently of mitochondrial fusion.

As Mgm1 and OPA1 are required for the assembly of the ATP synthase (Amutha *et al*, 2004; Gomes *et al*, 2011), we asked whether this assembly is modified by energy substrate availability and in a fusion-independent fashion. To this end, Blue-Native PAGE (BN-PAGE) was performed on isolated mitochondria treated with substrates affecting OPA1 oligomerization and cytochrome *c* retention. When mitochondria are fed with complex I substrates, which decrease OPA1 oligomers (Fig 2), both ATP synthase oligomers and monomers are decreased (Fig 5A), without a decrease in ATP5A subunits themselves (Fig 5B). BN-PAGE analysis in whole cells demonstrated that in WT MEFS, all ATP synthase subunits were assembled to form the monomer (very little dimer was detected); however, OPA1 KO MEFs had substantially less assembled ATP synthase monomers and an increase in free F_1 (Fig 5C). Reconstitution with either WT OPA1 or OPA1(Q297V) increased ATP synthase assembly, most notably when cells were forced to rely on OXPHOS for ATP production (galactose media, Fig 5C and D). While WT OPA1 completely rescued the assembly of the F_1 portion into F_1F_o monomers, OPA1(Q297V) cells still exhibited a significant level of free F_1, even in galactose media (Fig 5C and D). The persistence of free F_1 correlated with the inability of OPA1(Q297V) to rescue the loss of mtDNA caused by OPA1 deletion (Fig 5E), consistent with the requirement of mitochondrial fusion for mtDNA maintenance (Chen *et al*, 2010). While all of the subunits of the F_1 are nuclear-encoded, the F_o portion contains two subunits, ATP6 and ATP8, encoded by mtDNA. Since OPA1 KO and OPA1(Q297V) cells have decreased mtDNA levels, unassembled F_1 is likely due to a lack of mitochondrial-encoded F_o subunits. Interestingly, human mutations affecting expression of both mtDNA F_o subunits demonstrate increased free F_1 relative to monomer by BN-PAGE (Jonckheere *et al*, 2008; Pitceathly *et al*, 2012). Indeed, decreased levels of the mtDNA-encoded F_o subunit ATP6 in OPA1 KO and OPA1(Q297V) cells were confirmed by RT–PCR (Fig 5F). Since the OPA1(Q297V) mutant was unable to rescue mtDNA or mtDNA-encoded transcripts, here we propose a novel fusion-independent role of OPA1 on ATP synthase stability. Thus, assembly of a functional F_1F_o monomer depends dually on OPA1 for its stability and for fusion-dependent, mtDNA-encoded F_o subunit expression (Fig 5G).

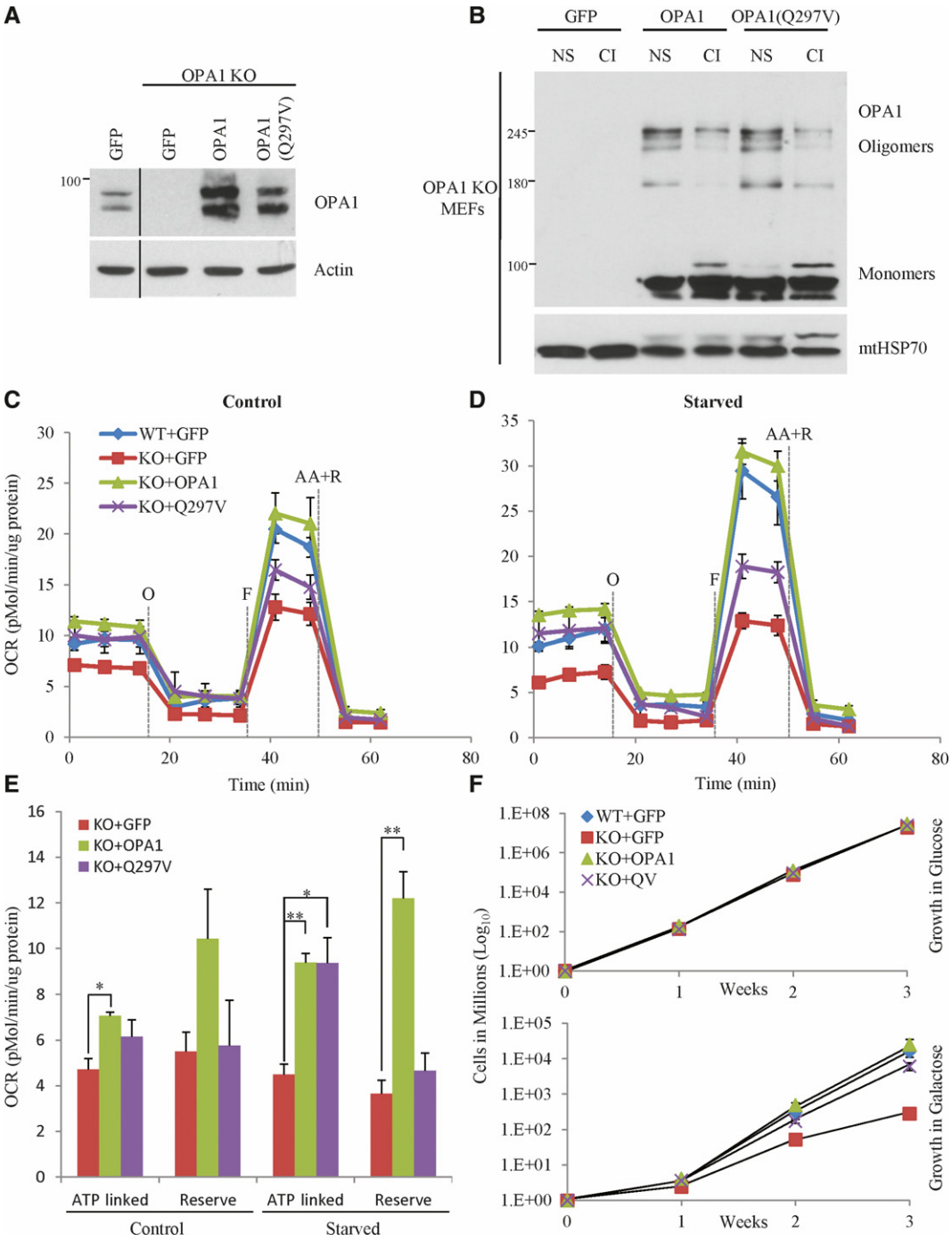

Figure 4. OPA1 regulates mitochondrial metabolism independently of mitochondrial fusion.

A WT and OPA1 knockout MEFs were infected with viruses encoding GFP, OPA1 or OPA1(Q297V) with dual promoters expressing GFP to allow for puromycin selection and FACS sorting cells for GFP expression. The resulting cultures were lysed, analysed by Western blot analysis and used for all subsequent experiments.

B OPA1 oligomers were analysed from isolated mitochondria incubated with no substrate or complex I substrates.

C, D To assess the impact of the fusion-incompetent OPA1 mutant on mitochondrial bioenergetics, we studied cells in the Seahorse XF-24 analyzer. Cells were plated on Seahorse TC plates 24 h prior to analysis, washed and incubated for 15 min in modified KRB and analysed. Cells in (D) were pre-starved for 2 h before analysis. At the indicated times, oligomycin (O), FCCP (F) and antimycin A (AA) with rotenone (R) were injected (averages ± SEM of three independent experiments).

E Quantification of ATP-linked OCR (resting OCR minus oligomycin-insensitive OCR) and reserve OCR (maximal minus resting) in (C) and (D).

F Long-term cell cultures were grown in glucose (top panel) or galactose media (bottom panel). Cells were passaged as required, medium was changed every 3 days if required, and cell number was determined once per week (averages ± SEM of four independent experiments).

Data information: Student's *t*-tests were performed relative to control, $*P < 0.05$ $**P < 0.01$.
Source data are available online for this figure.

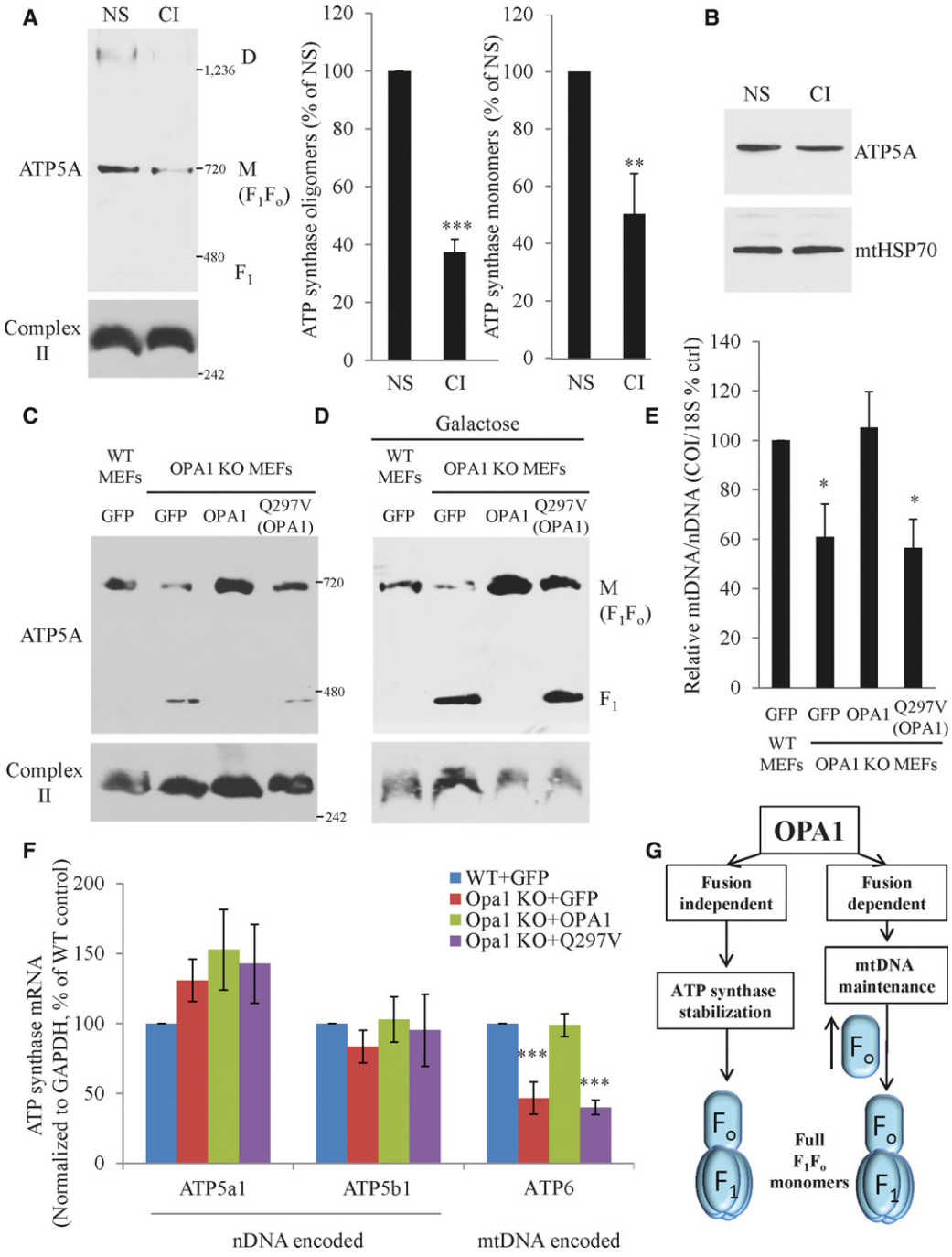

Figure 5. The dual role of OPA1 in regulating the ATP synthase.

A Isolated mitochondria incubated with complex I substrates were analysed by BN-PAGE and blotted for ATP5A of the ATP synthase. The oligomers [mostly dimers (D)] and monomer (M) of the ATP synthase were quantified as relative to complex II monomer (averages ± SEM of five independent experiments).

B Isolated liver mitochondria incubated with or without complex I in parallel with (A), lysed and analysed for ATP5A by straight Western blot.

C, D Long-term cultures of control cells (C) or cells grown for 1–2 weeks in galactose (D) were extracted for BN-PAGE directly from cells and blotted for ATP5A and complex II.

E DNA was extracted from long-term cultures, and mtDNA was analysed by qPCR relative to nDNA (averages ± SEM of three independent experiments).

F RNA was extracted from long-term cultures, and nuclear and mtDNA-encoded ATP synthase transcripts were analysed by RT–PCR (averages ± SEM of four independent experiments).

G Schematic diagram demonstrates the dual roles of OPA1 on the F_1F_o ATP synthase where OPA1 regulates the stabilization of the ATP synthase independently of its fusion activity and regulates mtDNA stability which is required for ATP6 (F_o subunit) expression and thus full F_1F_o ATP synthase assembly.

Data information: Student's *t*-tests were performed relative to control, $^*P < 0.05$, $^{**}P < 0.01$ and $^{***}P < 0.005$.
Source data are available online for this figure.

Solute carriers interact with OPA1 and regulate its sensing of mitochondrial energy substrates

Our results revealed that OPA1 responds to changes in fuel substrate conditions by modifying its oligomerization and that this is required for the adaptation and survival of cells during starvation. To determine the mechanism by which substrate levels modify OPA1 function, we performed a proteomics screen in search of OPA1 interacting factors. Stable isotope labelling of amino acids in cell culture (SILAC) combined with immunoprecipitation and mass spectroscopy was used as a quantitative and sensitive technique to identify novel OPA1 protein interactors that may be required for substrate sensing (Trinkle-Mulcahy, 2012) (Supplementary Fig S6A). A log SILAC ratio of 1 was set as the cut-off for validation since it gave a confidence interval of 95% (Supplementary Fig S6B). Of the 35 hits above a log SILAC ratio of 1, 18 (51%) were mitochondrial, 8 were ribosomal and 9 were either unknown or neither mitochondrial nor ribosomal (Supplementary Fig S6 and Supplementary Table S1). Highly relevant to fuel substrate sensing, a number of mitochondrial carrier proteins (SLC25A) were identified as OPA1-interacting proteins. Mitochondrial solute carriers are mitochondrial inner membrane proteins that catalyze the transfer of diverse substrates across the mitochondrial inner membrane [for a review see (Palmieri, 2013)]. Importantly, some of these solute carriers are involved in shuttling the mitochondrial substrates utilized in Fig 2, namely malate and succinate by SLC25A10 [the dicarboxylate carrier (DIC)], malate by SLC25A11 [the oxoglutarate carrier (OGC)] and glutamate by SLC25A12 and SLC25A13 [the aspartate/glutamate carriers 1 (AGC1) and 2 (AGC2)]. Given the requirement for OPA1-mediated cristae regulation in response to starvation, we asked whether these solute carriers were responsible for modulating OPA1 in response to substrate concentrations.

To first validate the OPA1–SLC25A protein interactions, C-terminally 3×flag-tagged solute carrier protein constructs (AGC1, AGC2, OGC and DIC) were overexpressed in MEFs and their mitochondrial localization was confirmed by immunofluorescence (Supplementary Fig S7A). Immunoprecipitation of tagged AGC1, AGC2, OGC and DIC revealed an interaction with endogenous OPA1 (Fig 6A), in line with the SILAC experiment where tagged OPA1 immunoprecipitated endogenous SLC25A proteins. Furthermore, immunoprecipitation of endogenous OPA1 from both isolated MEF and liver mitochondria also revealed an interaction with endogenous OGC but not other control mitochondrial proteins (Fig 6B, Supplementary Fig S7B). In addition, the interaction between OPA1 and OGC was decreased by 59.4% ± 10.7 (SEM, $n = 3$) when an OGC competitive inhibitor (phenylsuccinate) was added to the immunoprecipitation buffer suggestive of a dynamic interaction (Fig 6B, Supplementary Fig S7B). To further study this interaction and the role of solute carriers in the regulation of OPA1 assembly and function, we used both a genetic and pharmaceutical approach. To deplete OGC, MEFs were subjected to two rounds of siRNA transfection for a total of 120 h (Fig 6C). Neither OGC depletion nor OGC overexpression had an observable effect on mitochondrial length (Supplementary Fig S8A and B). In addition to mitochondrial length, OGC depletion had no effect on gross mitochondrial structure (Supplementary Fig S9A), OCR rates in regular growth conditions (Fig 6F and H) or cell survival in starvation (Supplementary Fig S9B and C), indicating that decreasing OGC levels does not disrupt overall mitochondrial structure and function. As our hypothesis is that OGC and other SLC25A proteins regulate OPA1 under changing substrate levels, we then measured the response of siOGC mitochondria to substrate availability *in vitro*. Incubation of siOGC mitochondria in the absence of substrates reduced OPA1 oligomerization, also reducing the difference in OPA1 oligomerization between fed and no substrate conditions (Fig 6D, Supplementary Fig S9D). Additionally, when isolated mitochondria were incubated in the absence of energy substrates, siOGC mitochondria were unable to retain as much cytochrome *c*, indicative of their inability to respond to changing substrate levels (Fig 6E, Supplementary Fig S9C). Next, we investigated the consequences of OGC depletion on the response to starvation. Starvation of siOGC cells significantly reduced their ATP-linked oxygen consumption rate (Fig 6G and H), indicating an impaired response to changes in substrate availability. In addition, siOGC cells displayed a modest but reproducible decrease in cell growth in galactose media (Fig 6I). These results indicate that OGC plays a role in the adaptation of mitochondria to changing energy substrate levels, possibly by regulating OPA1 oligomerization.

To confirm that OPA1 senses substrate availability through the SLC25A proteins, we utilized competitive inhibitors of the DIC and OGC in order to mimic substrate binding in the complete absence of actual energy substrates. Strikingly, both the DIC inhibitor butylmalonate (BM) and the OGC inhibitor phenylsuccinate (PhS) alone drastically reduced OPA1 oligomerization, mirroring the OPA1 response to substrate-rich conditions (Fig 7A). Again, this correlated with increased mobilization of cytochrome *c* stores, indicative of an increased cristae width (Fig 7B). Finally, since OPA1 regulates ATP synthase stability, we investigated the effect of the SLC25A inhibitors on the ATP synthase. Strikingly, both the dimer and the monomer of the ATP synthase were drastically decreased following incubation with BM or PhS (Fig 7C). Importantly, the decrease in ATP synthase and increase in cytochrome *c* mobilization were specific, as cytochrome *c* was not mobilized in the absence of digitonin (Fig 7B), complex II was not altered (Fig 7C), and BM and PhS did not alter total ATP5A levels (Fig 7D).

Altogether, these results indicate that OPA1 responds to changes in fuel substrate levels, influenced by SLC25A proteins, altering mitochondrial function through its role in cristae regulation and ATP synthase assembly.

Discussion

Cristae structural changes have been documented decades ago (Hackenbrock, 1966, 1968a,b), but our understanding of how these changes occur and their functional consequence is largely unknown. Here, we demonstrate a novel mechanism by which cristae are physiologically regulated. Changes in energy substrate availability are sensed by mitochondrial SLC25A transporters, which in turn regulate OPA1 oligomerization. OPA1 oligomerization is then required to modulate cristae width and regulate assembly of the ATP synthase, in a mitochondrial fusion-independent manner. The physiological importance of this mechanism is highlighted by the demonstration that a fusion-incompetent form of OPA1(Q297V) rescued OCR, ATP synthase assembly and cell growth of OPA1 KO MEFs in galactose media, which forces mitochondrial respiration for ATP production.

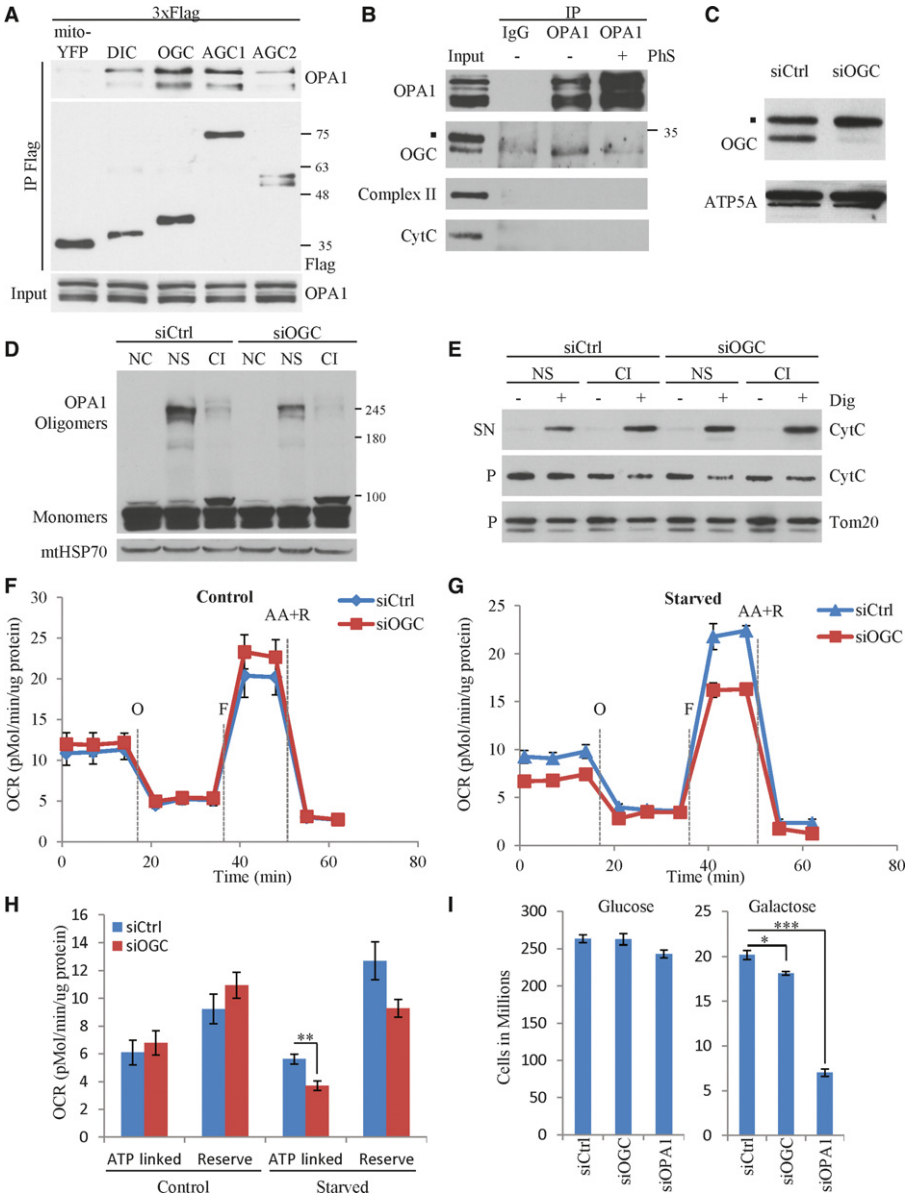

Figure 6. OPA1 interacts with SLC25 proteins that regulate OPA1's response to starvation.

A Mito-YFP-3×flag, DIC-3×flag, OGC-3×flag, AGC1-3×flag and AGC2-3×flag constructs were transiently transfected into MEFs. Twenty-four hours post-transfection, cells were lysed, immunoprecipitated with anti-flag antibodies and analysed by Western blot.

B Endogenous OPA1 was immunoprecipitated from MEF mitochondrial lysates with or without 15 mM phenylsuccinate (PhS), and the eluted samples were analysed by Western blot. Complex II and cytochrome *c* were used as negative controls.

C Representative OGC knockdown for experiments in (D-H) (see also Supplementary Figs S8B and S9A–E). MEFs were transfected twice with siOGC for 120 h total, and mitochondrial lysates were analysed by Western blot.

D Isolated mitochondria from siOGC-treated cells were incubated with the indicated ETC substrates (NC: non-crosslinked control; NS: no substrate control; CI: complex I, malate and glutamate at 5 mM each) for 30 min at 37°C and crosslinked with EDC, and OPA1 oligomers were then analysed by gradient gel Western blot.

E Isolated mitochondria from siOGC and siCtrl cells were incubated in no substrate or complex I buffers for 30 min and analysed for cytochrome *c* retention.

F, G SiOGC and siCtrl cells were plated onto Seahorse TC plates 24 h prior to analysis, washed and incubated for 15 min in modified KRB and analysed by the XF analyzer. Cells in (G) were pre-starved for 2 h before analyses. At the indicated times, oligomycin (O), FCCP (F) and antimycin A (AA) with Rotenone (R) were injected.

H Quantification of ATP-linked (resting OCR minus oxygen leak) and reserve OCR (maximal minus resting OCR) in (F) and (G) (averages ± SEM of four independent experiments).

I MEFs were grown for 1 week in galactose media, to revert to a more oxidative phenotype, or in regular glucose media, and these cells (1×10^6) were transfected with either siCtrl, siOGC or siOPA1 and maintained in their respective media. Cells were then left to grow, passaged when required, and cell number in regular growth medium (left panel) or galactose media (right panel) was counted 6 days later (averages ± SEM of 4 independent experiments).

Data information: Student's *t*-tests were performed as indicated: $*P < 0.05$, $**P < 0.01$, $***P < 0.005$. ▪ indicates a background band in (B) and (C).
Source data are available online for this figure.

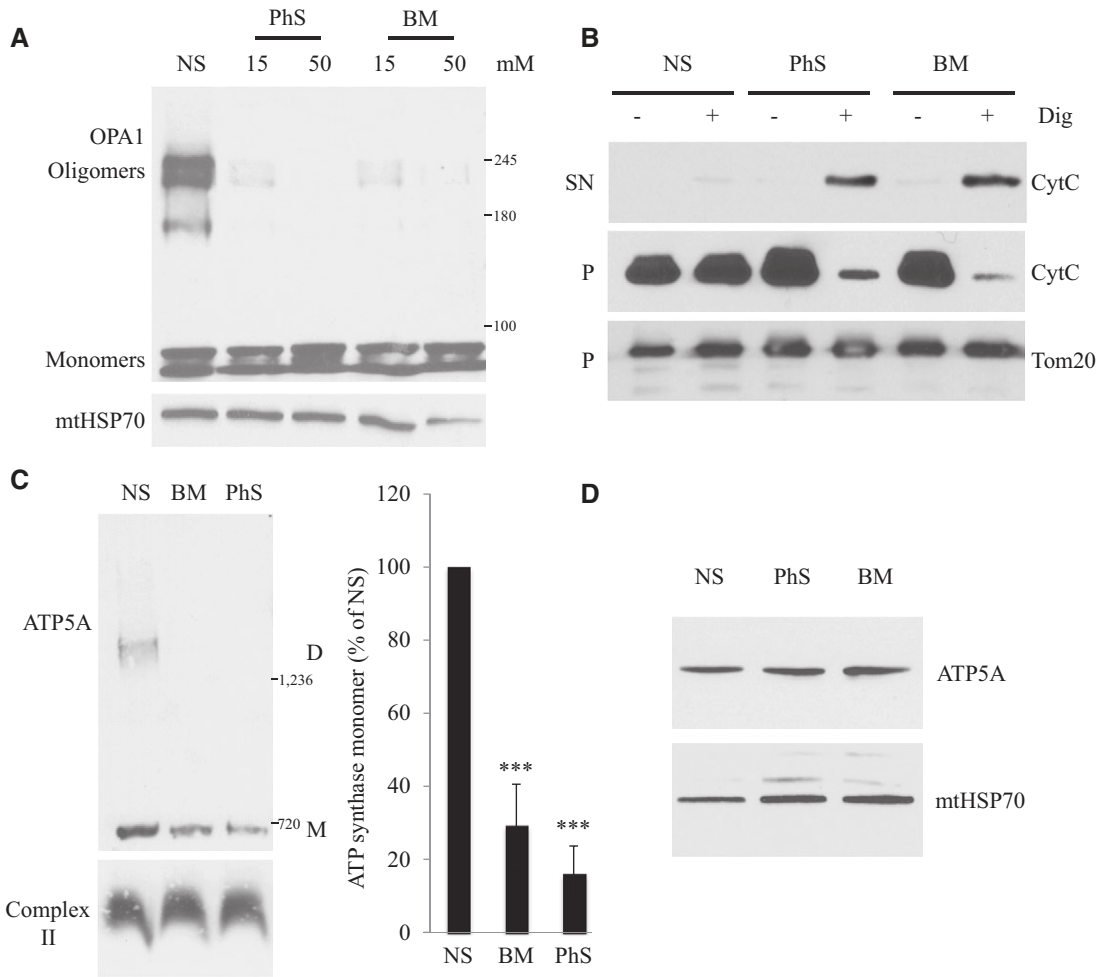

Figure 7. Pharmacological blockade of SLC25A proteins drastically inhibit OPA1 oligomerization and function.

A Isolated liver mitochondria were incubated with phenylsuccinate (PhS) or butylmalonate (BM), and OPA1 oligomerization was assessed as previously.

B Mouse liver mitochondria were incubated with 50 mM PhS or BM, and then, cytochrome *c* retention was analysed where released CytC was mobilized from the pellet (P) to the supernatant (SN) fraction.

C Mouse liver mitochondria were incubated with 50 mM PhS or BM, and lysates were analysed by BN-PAGE. ATP synthase monomers were quantified (right panel) relative to complex II monomer (averages ± SEM of 6 independent experiments).

D Mouse liver mitochondria were prepared and incubated in parallel with 7C and analysed by regular Western blot for ATP5A.

Data information: Student's *t*-tests were performed relative to control, ***$P < 0.005$.
Source data are available online for this figure.

Although it is known that OPA1 oligomers disassemble during cell death leading to release of proapoptotic factors (Frezza *et al*, 2006) and that OPA1 oligomer disruption by cristae remodelling results in impaired respiration (Cogliati *et al*, 2013), physiological changes in OPA1 oligomers and their role in regulating cristae structure under non-cell death conditions remained poorly understood. Here, we demonstrated in both cells and isolated mitochondria that starvation increases OPA1 oligomers rapidly and reversibly, correlating with tighter cristae width. These substrate-dependent changes in OPA1 oligomers were upstream/independent of ETC function and membrane potential, known regulators of OPA1 processing and its fusion function (Song *et al*, 2007; Mishra *et al*, 2014). By taking advantage of the OPA1(Q297V) mutant, we showed that, independently of mitochondrial fusion, OPA1 can maintain cristae structure and mitochondrial activity and adapt to the lack of nutrients during starvation. Our study therefore demonstrates that the roles of OPA1 in mitochondrial fusion and cristae maintenance can be separated and that cristae can be maintained in the absence of mitochondrial fusion.

How oligomerized OPA1 regulates cristae structure is still largely unknown. One proposed mechanism is through the oligomerization of two long and one short isomer of OPA1 (Frezza *et al*, 2006), although OPA1 oligomerization could also promote its interaction with other protein complexes required for cristae formation. In support of this hypothesis, our SILAC-based interaction screens revealed interactions with several factors critical for cristae structure maintenance: the ATP synthase, prohibitin, mitofilin, CHCHD3, Sam50 and the adenonucleotide transporters. In fact, recent groundbreaking studies have revealed protein complexes required for cristae maintenance termed MINOS, MitOS or MICOS (Harner *et al*, 2011; Hoppins *et al*, 2011; von der Malsburg *et al*, 2011). Indeed,

disruption of these components may lead to cristae loss, decreased ETC complexes and a decrease in respiration. In addition, since it has been demonstrated that ATP synthase oligomerization mediates cristae morphogenesis (Paumard *et al*, 2002; Habersetzer *et al*, 2013), it is possible that OPA1 oligomer-dependent changes regulate the ATP synthase which then alters cristae structure. In any case, the fact that OPA1 interacts with cristae maintenance components, as well as the ATP synthase, highlights its central role in the coordinated regulation of mitochondrial structure and function.

One of the ways in which cristae structure may regulate ETC function is by controlling local substrate concentrations. From computer modelling experiments, it has been proposed that these changes in cristae structure may regulate the diffusion of metabolites (Mannella, 2006b). Scorrano's group has shown that OPA1 is required for the regulation of respiratory chain supercomplex assembly (Cogliati *et al*, 2013). These ETC supercomplexes may increase the efficiency of electron transfer and ATP production and may decrease the toxic accumulation of reactive oxygen species (Wittig & Schagger, 2009; Lenaz & Genova, 2012). Here, we present non-cell death manipulations of healthy cells or mitochondria to demonstrate that OPA1 regulates ATP synthase expression and the stabilization of the functional monomer, independently of OPA1 fusion activity. The starvation-induced rescue of ATP synthase assembly by OPA1 and OPA1(Q297V) clearly supports a major role for these complexes in fine-tuning mitochondrial function according to nutrient availability. However, we cannot exclude that part of the prosurvival role of OPA1(Q297V) is in preventing the release of proapoptotic factors from mitochondria, as previously suggested under apoptotic conditions (Yamaguchi *et al*, 2008). Interestingly, the OPA1(Q297V) mutant still responds to changes in fuel substrate availability without GTPase activity, potentially mimicking GTP binding (Yamaguchi *et al*, 2008), suggesting that OPA1 oligomerization is upstream of GTP binding and hydrolysis.

We identified members of the SLC25A family of mitochondrial solute carriers being required for OPA1 oligomerization in response to changes in energy substrate levels. Since their pharmacological and genetic ablation resulted in disruption of OPA1 oligomers and cytochrome *c* mobilization, outside of transporting their respective substrates, SLC25As could represent a novel class of inner membrane-shaping proteins. While our results suggest that OGC interacts with OPA1, we cannot exclude the possibility that it affects OPA1 indirectly, by modulating some undefined mitochondrial process. Moreover, the mechanism governing how SLC25A proteins transport their cargo as well as relay information to OPA1 still remains to be determined. Work on other more characterized solute carriers, the amino acid transporters, suggests that they may act as sensors in addition to carrier functions by activating different cellular signalling pathways [reviewed in (Taylor, 2014)]. The transfer of this idea to SLC25A proteins is of interest, considering the effect of OGC depletion and SLC25 inhibition on OPA1 oligomerization and function. Additionally, since the effect on OPA1 oligomerization and cytochrome *c* mobilization with these drugs was so robust, it would be interesting to investigate whether targeting SLC25As represent a novel mechanism to adjust the cell death programme.

In conclusion, we propose a model in which OPA1 senses the presence of mitochondrial fuel substrates upstream and independently of ETC activity itself. These substrates lead to OPA1 oligomerization and tightening of cristae. These ultrastructural changes are accompanied by increased assembly of the ATP synthase which promotes the efficiency or capacity for ATP produced by oxidative phosphorylation. We believe that these cristae structural changes may be required for other physiological adaptations, which warrants further investigation. Finally, our findings strengthen the link between OPA1 and cristae maintenance and suggest another mechanism by which the cell can respond to its metabolic supply.

Materials and Methods

Cell culture, transfections and viral production

HeLa and MEF cells were cultured in DMEM supplemented with 10% FBS (Wisent), 50 μg/ml penicillin and streptomycin and 2 mM glutamine (Gibco). Galactose media were prepared from glucose-/pyruvate-free DMEM supplemented as above with 10 mM galactose (Sigma). Cells were transfected using Lipofectamine 2000 (Invitrogen) or with the indicated siRNA using siLentFect (Bio-Rad) according to the manufacturer's protocol. Viral vectors were prepared as previously described (Tashiro *et al*, 2006; Jahani-Asl *et al*, 2011). All constructs used are listed in Supplementary Table S2.

To generate the long-term expression cultures, OPA1 KO cells were infected with viruses encoding for WT OPA1, OPA1(Q297V) or GFP as control and WT cells were infected with control GFP. Following transduction, cells were selected with puromycin and FACS sorted for GFP expression. These cell lines were maintained and used between 4 and 12 weeks after stable expression for all experiments.

Mitochondrial isolation

Mouse liver was dissected from young CD-1 or C57BL/6 mice euthanized with sodium pentobarbital. Cells or mouse liver were rinsed with PBS and lysed in mitochondrial isolation buffer (200 mM mannitol, 70 mM sucrose, 10 mM HEPES, pH 7.4, 1 mM EGTA). The isolation was performed in its entirety on ice or at 4°C. Cells were homogenized with a 25-G needle 15 times, while liver was Dounce-homogenized 10 times. Nuclei and cell debris were pelleted by centrifugation at 1,000 rpm for 9 min. The supernatant was then centrifuged at 9,000 rpm for 9 min to pellet mitochondria. These two spins are repeated to further enrich mitochondria in this heavy membrane fraction. Mitochondrial purity was confirmed by Western blot and EM.

Western blot analysis

Western blots were performed as previously described (Germain *et al*, 2013), with the following antibodies: mouse anti-actin and anti-flag (Sigma-Aldrich); mouse anti-OPA1 and anti-cytochrome *c* (BD Bioscience); mouse anti-p62 (SQSTM1) and rabbit anti-TOM20 (Santa Cruz Biotechnologies); mouse anti-ATP5A and anti-Complex II (Invitrogen); and mouse anti-mtHSP70 (ABR Bioreagents) and rabbit anti-OGC (Abcam).

Analysis of OPA1 oligomers

To analyse rapid changes in OPA1 oligomerization in whole cells, we used the cell-permeable BMH (Thermo Scientific) (1 mM) for

20 min at 37°C. After crosslinking, cells were quenched and washed in PBS with 0.1% beta-mercaptoethanol (BME) twice. Cells were then lysed in lysis buffer with BME and subjected to Western blot on NuPAGE Novex 3–8% Tris-acetate gradient gels (Life Technologies). For mitochondrial experiments, isolated liver or MEF mitochondria were suspended in the indicated buffer (200 mM sucrose, 10 mM Tris-Mops pH 7.4, 2 mM K_2HPO_4, 0.080 mM ADP, 10 μM EGTA-Tris) at 0.5–1 μg of mitochondrial protein/μl. Substrates and drugs were also added or not as follows: malate, glutamate, succinate and glucose (5 mM) (Sigma); rotenone (2 μM) (Sigma); and carbonylcyanide-3-chlorophenylhydrazone (CCCP) (10 μM) (Sigma). All drugs and substrates were adjusted to pH 7.4. Samples were then incubated on a 37°C heating block for 30 min or 1 h. After incubation, EDC (1 mM) (Thermo Scientific) or BMH (10 mM) was added for 30 min at room temperature and quenched with BME. Samples were then analysed by gradient gel Western blot.

Cytochrome *c* retention assay

As a read-out for changes in mitochondrial ultrastructure, mitochondria were assayed for their ability to retain cytochrome *c*. Mitochondria were incubated as described and then incubated with low digitonin (1 mg/mg of protein at 0.1%), at 4°C for 30 min to mobilize their inner cristae stores dependent on cristae ultrastructure. Mitochondria are then centrifuged for 10 min at 10,000 rpm (4°C) to separate the released proteins. The resulting supernatants and pellets (volume equivalents from 12.5 μg of starting mitochondria) were analysed by Western blot.

Immunofluorescence and cell death assays

Cells were washed twice with PBS and fixed with 4% paraformaldehyde for 20 min and analysed with the indicated primary antibodies. Coverslips were then washed and incubated with their corresponding secondary antibodies (anti-mouse and anti-rabbit Alexa Fluor 488/Alexa Fluor 594). Hoechst stain (Sigma) was added with the secondary antibody where noted to visualize the nucleus. Coverslips were then washed and mounted using Gel Mount Aqueous mounting medium (Sigma).

To analyse cell death during starvation, 24 h after transfection, cells were starved for 6 h and stained using propidium iodide (PI) and Hoescht stain for 20 min. All dead (Pi^+) were counted and expressed as a percentage of all cells ($Hoescht^+$). Cell death was also quantified as the percentage of condensed nuclei to total nuclei. Images were taken of at least six fields of view on a 20× objective, containing an average of 200 cells each (> 1,000 cells total).

Immunoprecipitations

Twenty-four hours following transfection, cells were lysed (50 mM Tris–HCl, 150 mM NaCl, 1 mM EDTA, 1% Triton X-100 and 1:1,000 PIC at pH 7.4), and proteins (2 mg) were immunoprecipitated with ANTI-FLAG M2 magnetic beads (Sigma-Aldrich) according to the manufacturers protocol. Samples were incubated overnight and the beads were washed four times with TBS (50 mM Tris–HCl, 150 mM NaCl and 1:1,000 PIC at pH 7.4). Immunoprecipitated protein was then eluted from the magnetic beads twice with elution buffer (50 mM Tris–HCl and 150 mM NaCl, at pH 7.4 containing 150 ng/μl FLAG peptides). Endogenous immunoprecipitation of OPA1 was performed on isolated MEF or liver mitochondria with CHAPS containing buffer (50 mM Tris–HCl, 150 mM NaCl, 1 mM EDTA, 1% CHAPS and 1:1,000 PIC at pH 7.4) at 4°C overnight with no antibody, normal mouse IgG, or mouse monoclonal anti-OPA1 (BD Biosciences). OPA1 complexes were then immunoprecipitated with 20 μl of A/G magnetic beads (Pierce) at RT for 1 h, washed with TBS four times, eluted with SDS loading dye for 20 min and analysed by Western blot.

Transmission electron microscopy

To analyse rapid cristae structure changes during cell starvation, cells were adhered to square glass coverslips, grown to confluence, treated and rapidly fixed with a combination of 2% paraformaldehyde and 1.6% glutaraldehyde. Fixed cells were floated off their cover slips, and samples were processed as previously described (Jahani-Asl *et al*, 2011). For structural quantification, the cristae diameter and mitochondrial width were measured from all mitochondria from ten cells for each condition in two independent cultures. For analysis of cristae structure in isolated mitochondria, mitochondria were treated as indicated, fixed with 2% glutaraldehyde for 20 min at RT and analysed by EM.

Blue-native analysis of ETC complexes

ATP synthase assembly was analysed from whole cells and isolated mitochondria by Blue-Native PAGE (BN-PAGE) electrophoresis according to Wittig *et al* (2006). The digitonin extraction and BN-PAGE electrophoresis were performed entirely on ice or at 4°C. Cells were grown on 100-mm plates, washed with PBS and scraped in PBS. Cells were pelleted at 3,000 rpm for 5 min, or mitochondria were pelleted at 9,000 rpm for 9 min and resuspended in digitonin extraction buffer (50 mM imidazole/HCl pH 7.0, 50 mM NaCl, 5 mM 6-aminohexanoic acid, 1 mM EDTA with 1% digitonin). Final protein to digitonin ratios were 1:4 w/w for cells and 1:8 w/w for mitochondria. Protein was extracted on ice for 1 h (for cells) or 30 min (for mitochondria) and cleared at 14,000 rpm for 30 min. Protein was quantified and 150 μg of protein (or 75 μg from mitochondria) was loaded with 5% glycerol and 1:10 dye:digitonin ratio of Coomassie blue G-250 in 500 mM 6-aminohexanoic acid onto home-made 3–13% large gels. Gels were run 2 h in a high Coomassie blue G-250 cathode buffer at 150 V at 4°C and then switched to a low G-250 buffer overnight at 4°C. Pictures of the gels were taken to confirm proper loading, and gels were transferred to nitrocellulose membrane at 500 mA for 2 h. The resulting membranes were Western blotted as per above.

mtDNA and mRNA quantification

DNA was extracted by phenol–chloroform–isoamylalcohol extraction according to Guo *et al* (2009), followed by qPCR with SYBR Green FastMix (Quanta Biosciences) according to the manufacturer's protocol with the indicated primers in Supplementary Table S2. RNA was extracted with TRIzol (Life Technologies) and analysed by RT–PCR according to Gomes *et al* (2013) with the indicated primers in Supplementary Table S2.

Analysis of oxygen consumption rates

To assess mitochondrial respiration, oxygen consumption was measured with the XF24 Analyzer (Seahorse Biosciences). Cells (50,000 experimentally optimized) were seeded onto 24-well XF24 cell culture plates. On the following day, cells were starved or not for 2 h. Cells were then washed and incubated with modified Kreb's Ringer Buffer (KRB) (KRB: 128 mM NaCl, 4.8 mM KCl, 1.2 mM KH_2PO_4, 1.2 mM $MgSO_4$, 25 mM $CaCl_2$, 0.1% BSA (fatty acid free); completed on the day of the experiment with 10 mM glucose and 1 mM sodium pyruvate and pH 7.4) for 15 min at 37°C prior to cartridge loading in the XF Analyser. Following resting respiration, cells were treated sequentially with: oligomycin (0.2 μg/μl), for nonphosphorylating OCR; FCCP (1 μM), for maximal OCR; and antimycin A (2.5 μM) with rotenone (1 μM), for extramitochondrial OCR. Measurements were taken over 2-min intervals, proceeded by a 2-min mixing and a 2-min incubation. Three measurements were taken for the resting OCR, three for nonphosphorylating OCR, two for maximal OCR and two for extramitochondrial OCR. All data were compiled by the XF software, normalized to protein levels per well and analysed with Microsoft Excel.

Stable isotope labelling with amino acids in cell culture (SILAC) coupled Immunoprecipitation and mass spectrometry

SILAC-coupled immunoprecipitation and MS was performed as previously described (Trinkle-Mulcahy, 2012). HeLa cells were grown in DMEM minus arginine and lysine, supplemented with 10% dialysed FBS, 100 U/ml penicillin/streptomycin and either 'light' L-arginine and L-lysine or 'heavy' L-arginine ^{13}C and L-lysine 4,4,5,5-D4. Cells were grown and passaged for 10 days to allow for incorporation of isotopic amino acids. Cells were then transduced with control adenovirus (mito-YFP) in the light conditions and with OPA1-YFP adenovirus in the heavy condition. Cells were harvested 24 h after transduction and lysed in RIPA buffer (50 mM Tris–HCl pH 7.5, 150 mM NaCl, 1% NP-40, 0.5% deoxycholate and protease inhibitors). Proteins were immunoprecipitated with GFP-Trap_A (Chromotek) and combined during immunoprecipitation washes and eluted together. Proteins were then reduced with 10 mM DTT, alkylated with 50 mM iodoacetamide and separated on pre-cast SDS–PAGE gels (Invitrogen). Bands were cut and digested with trypsin, and peptides were recovered. Peptides were analysed by liquid chromatography–mass spectrometry (LC-MS) using an LTQ-Oribitrap mass MS system coupled to a Dionex 3000 nano-LC system. Raw data files were analysed using the UniProt human database. Quantitation was performed using the MaxQuant software package (Cox & Mann, 2008). Positive OPA1 interactors were identified as being enriched in the heavy condition.

Supplementary information for this article is available online: http://emboj.embopress.org

Acknowledgments

We would like to acknowledge Peter Rippstein from the Ottawa Heart Institute for the preparation of EM samples as well as technical assistance, Delphine Chamousset for technical assistance with SILAC experiments, Dr. Ilona Skerjanc for essential equipment and Delphie Dugal-Tessier for reviewing the manuscript. WT and OPA1 KO MEFs were a kind gift from Dr. Luca Scorrano.

This work was supported by grants to R.S.S. from the Canadian Institutes of Health Research (MOP50471), the Heart and Stroke Foundation of Canada (T7185) and the Brain Canada/Krembil Foundation, and by a grant to ME.H. from the Canadian Institutes of Health Research (MOP57810). D.A.P. was supported by scholarships from the Shelby Hayter Pass the Baton Graduate Fellowship from the Parkinson's Research Consortium, Ontario Graduate Scholarship and a Focus on Stroke Doctoral Research Award from the Heart and Stroke Foundation. M.G. was supported by a Parkinson's Society of Canada Research Fellowship. J.W. was supported by a Ontario Graduate Scholarship. M.K. was supported by a Focus on Stroke Fellowship from the Heart and Stroke Society of Canada.

Author contributions

DAP and RSS performed conception and design of experiments, data acquisition, analysis and interpretation of data, and drafting and revising the manuscript. MG and JW contributed to the conception and design of experiments, data acquisition, analysis and interpretation of data and revision of the manuscript. MK, VS and RM contributed to the design of experiments, interpretation of data and revision of the manuscript. KPL contributed to the design of experiments, data acquisition and interpretation of results. JM contributed to the design of experiments and data acquisition. DSP, HM, LTM and MEH contributed to the design of experiments, contributed critical reagents and revised the manuscript.

Conflict of interest

The authors declare that they have no conflict of interest.

References

Aguer C, Gambarotta D, Mailloux RJ, Moffat C, Dent R, McPherson R, Harper ME (2011) Galactose enhances oxidative metabolism and reveals mitochondrial dysfunction in human primary muscle cells. *PLoS ONE* 6: e28536

Alexander C, Votruba M, Pesch UE, Thiselton DL, Mayer S, Moore A, Rodriguez M, Kellner U, Leo-Kottler B, Auburger G, Bhattacharya SS, Wissinger B (2000) OPA1, encoding a dynamin-related GTPase, is mutated in autosomal dominant optic atrophy linked to chromosome 3q28. *Nat Genet* 26: 211–215

Amutha B, Gordon DM, Gu Y, Pain D (2004) A novel role of Mgm1p, a dynamin-related GTPase, in ATP synthase assembly and cristae formation/maintenance. *Biochem J* 381: 19–23

Chen H, Detmer SA, Ewald AJ, Griffin EE, Fraser SE, Chan DC (2003) Mitofusins Mfn1 and Mfn2 coordinately regulate mitochondrial fusion and are essential for embryonic development. *J Cell Biol* 160: 189–200

Chen H, Vermulst M, Wang YE, Chomyn A, Prolla TA, McCaffery JM, Chan DC (2010) Mitochondrial fusion is required for mtDNA stability in skeletal muscle and tolerance of mtDNA mutations. *Cell* 141: 280–289

Cogliati S, Frezza C, Soriano ME, Varanita T, Quintana-Cabrera R, Corrado M, Cipolat S, Costa V, Casarin A, Gomes LC, Perales-Clemente E, Salviati L, Fernandez-Silva P, Enriquez JA, Scorrano L (2013) Mitochondrial cristae shape determines respiratory chain supercomplexes assembly and respiratory efficiency. *Cell* 155: 160–171

Cox J, Mann M (2008) MaxQuant enables high peptide identification rates, individualized p.p.b.-range mass accuracies and proteome-wide protein quantification. *Nat Biotechnol* 26: 1367–1372

Delettre C, Lenaers G, Griffoin JM, Gigarel N, Lorenzo C, Belenguer P, Pelloquin L, Grosgeorge J, Turc-Carel C, Perret E, Astarie-Dequeker C,

Lasquellec L, Arnaud B, Ducommun B, Kaplan J, Hamel CP (2000) Nuclear gene OPA1, encoding a mitochondrial dynamin-related protein, is mutated in dominant optic atrophy. *Nat Genet* 26: 207 – 210

Frezza C, Cipolat S, Martins de Brito O, Micaroni M, Beznoussenko GV, Rudka T, Bartoli D, Polishuck RS, Danial NN, De Strooper B, Scorrano L (2006) OPA1 controls apoptotic cristae remodeling independently from mitochondrial fusion. *Cell* 126: 177 – 189

Germain M, Mathai JP, McBride HM, Shore GC (2005) Endoplasmic reticulum BIK initiates DRP1-regulated remodelling of mitochondrial cristae during apoptosis. *EMBO J* 24: 1546 – 1556

Germain M, Nguyen AP, Khacho M, Patten DA, Screaton RA, Park DS, Slack RS (2013) LKB1-regulated adaptive mechanisms are essential for neuronal survival following mitochondrial dysfunction. *Hum Mol Genet* 22: 952 – 962

Gomes LC, Di Benedetto G, Scorrano L (2011) During autophagy mitochondria elongate, are spared from degradation and sustain cell viability. *Nat Cell Biol* 13: 589 – 598

Gomes AP, Price NL, Ling AJ, Moslehi JJ, Montgomery MK, Rajman L, White JP, Teodoro JS, Wrann CD, Hubbard BP, Mercken EM, Palmeira CM, de Cabo R, Rolo AP, Turner N, Bell EL, Sinclair DA (2013) Declining NAD(+) induces a pseudohypoxic state disrupting nuclear-mitochondrial communication during aging. *Cell* 155: 1624 – 1638

Guo W, Jiang L, Bhasin S, Khan SM, Swerdlow RH (2009) DNA extraction procedures meaningfully influence qPCR-based mtDNA copy number determination. *Mitochondrion* 9: 261 – 265

Habersetzer J, Larrieu I, Priault M, Salin B, Rossignol R, Brethes D, Paumard P (2013) Human F1F0 ATP synthase, mitochondrial ultrastructure and OXPHOS impairment: a (super-)complex matter? *PLoS ONE* 8: e75429

Hackenbrock CR (1966) Ultrastructural bases for metabolically linked mechanical activity in mitochondria. I. Reversible ultrastructural changes with change in metabolic steady state in isolated liver mitochondria. *J Cell Biol* 30: 269 – 297

Hackenbrock CR (1968a) Chemical and physical fixation of isolated mitochondria in low-energy and high-energy states. *Proc Natl Acad Sci USA* 61: 598 – 605

Hackenbrock CR (1968b) Ultrastructural bases for metabolically linked mechanical activity in mitochondria. II. Electron transport-linked ultrastructural transformations in mitochondria. *J Cell Biol* 37: 345 – 369

Harner M, Korner C, Walther D, Mokranjac D, Kaesmacher J, Welsch U, Griffith J, Mann M, Reggiori F, Neupert W (2011) The mitochondrial contact site complex, a determinant of mitochondrial architecture. *EMBO J* 30: 4356 – 4370

Hoppins S, Collins SR, Cassidy-Stone A, Hummel E, Devay RM, Lackner LL, Westermann B, Schuldiner M, Weissman JS, Nunnari J (2011) A mitochondrial-focused genetic interaction map reveals a scaffold-like complex required for inner membrane organization in mitochondria. *J Cell Biol* 195: 323 – 340

Jahani-Asl A, Pilon-Larose K, Xu W, MacLaurin JG, Park DS, McBride HM, Slack RS (2011) The mitochondrial inner membrane GTPase, optic atrophy 1 (Opa1), restores mitochondrial morphology and promotes neuronal survival following excitotoxicity. *J Biol Chem* 286: 4772 – 4782

Jonckheere AI, Hogeveen M, Nijtmans LG, van den Brand MA, Janssen AJ, Diepstra JH, van den Brandt FC, van den Heuvel LP, Hol FA, Hofste TG, Kapusta L, Dillmann U, Shamdeen MG, Smeitink JA, Rodenburg RJ (2008) A novel mitochondrial ATP8 gene mutation in a patient with apical hypertrophic cardiomyopathy and neuropathy. *J Med Genet* 45: 129 – 133

Lenaz G, Genova ML (2012) Supramolecular organisation of the mitochondrial respiratory chain: a new challenge for the mechanism and control of oxidative phosphorylation. *Adv Exp Med Biol* 748: 107 – 144

von der Malsburg K, Muller JM, Bohnert M, Oeljeklaus S, Kwiatkowska P, Becker T, Loniewska-Lwowska A, Wiese S, Rao S, Milenkovic D, Hutu DP, Zerbes RM, Schulze-Specking A, Meyer HE, Martinou JC, Rospert S, Rehling P, Meisinger C, Veenhuis M, Warscheid B *et al* (2011) Dual role of mitofilin in mitochondrial membrane organization and protein biogenesis. *Dev Cell* 21: 694 – 707

Mannella CA (2006a) The relevance of mitochondrial membrane topology to mitochondrial function. *Biochim Biophys Acta* 1762: 140 – 147

Mannella CA (2006b) Structure and dynamics of the mitochondrial inner membrane cristae. *Biochim Biophys Acta* 1763: 542 – 548

Meeusen S, DeVay R, Block J, Cassidy-Stone A, Wayson S, McCaffery JM, Nunnari J (2006) Mitochondrial inner-membrane fusion and crista maintenance requires the dynamin-related GTPase Mgm1. *Cell* 127: 383 – 395

Misaka T, Miyashita T, Kubo Y (2002) Primary structure of a dynamin-related mouse mitochondrial GTPase and its distribution in brain, subcellular localization, and effect on mitochondrial morphology. *J Biol Chem* 277: 15834 – 15842

Mishra P, Carelli V, Manfredi G, Chan DC (2014) Proteolytic cleavage of Opa1 stimulates mitochondrial inner membrane fusion and couples fusion to oxidative phosphorylation. *Cell Metab* 19: 630 – 641

Palmieri F (2013) The mitochondrial transporter family SLC25: identification, properties and physiopathology. *Mol Aspects Med* 34: 465 – 484

Paumard P, Vaillier J, Coulary B, Schaeffer J, Soubannier V, Mueller DM, Brethes D, di Rago JP, Velours J (2002) The ATP synthase is involved in generating mitochondrial cristae morphology. *EMBO J* 21: 221 – 230

Pitceathly RD, Murphy SM, Cottenie E, Chalasani A, Sweeney MG, Woodward C, Mudanohwo EE, Hargreaves I, Heales S, Land J, Holton JL, Houlden H, Blake J, Champion M, Flinter F, Robb SA, Page R, Rose M, Palace J, Crowe C *et al* (2012) Genetic dysfunction of MT-ATP6 causes axonal Charcot-Marie-Tooth disease. *Neurology* 79: 1145 – 1154

Rambold AS, Kostelecky B, Elia N, Lippincott-Schwartz J (2011) Tubular network formation protects mitochondria from autophagosomal degradation during nutrient starvation. *Proc Natl Acad Sci USA* 108: 10190 – 10195

Scorrano L, Ashiya M, Buttle K, Weiler S, Oakes SA, Mannella CA, Korsmeyer SJ (2002) A distinct pathway remodels mitochondrial cristae and mobilizes cytochrome *c* during apoptosis. *Dev Cell* 2: 55 – 67

Song Z, Chen H, Fiket M, Alexander C, Chan DC (2007) OPA1 processing controls mitochondrial fusion and is regulated by mRNA splicing, membrane potential, and Yme1L. *J Cell Biol* 178: 749 – 755

Sukhorukov VM, Bereiter-Hahn J (2009) Anomalous diffusion induced by cristae geometry in the inner mitochondrial membrane. *PLoS ONE* 4: e4604

Tashiro A, Zhao C, Gage FH (2006) Retrovirus-mediated single-cell gene knockout technique in adult newborn neurons in vivo. *Nat Protoc* 1: 3049 – 3055

Taylor PM (2014) Role of amino acid transporters in amino acid sensing. *Am J Clin Nutr* 99: 223S – 230S

Tondera D, Grandemange S, Jourdain A, Karbowski M, Mattenberger Y, Herzig S, Da Cruz S, Clerc P, Raschke I, Merkwirth C, Ehses S, Krause F, Chan DC, Alexander C, Bauer C, Youle R, Langer T, Martinou JC (2009) SLP-2 is required for stress-induced mitochondrial hyperfusion. *EMBO J* 28: 1589 – 1600

Trinkle-Mulcahy L (2012) Resolving protein interactions and complexes by affinity purification followed by label-based quantitative mass spectrometry. *Proteomics* 12: 1623 – 1638

Vogel F, Bornhovd C, Neupert W, Reichert AS (2006) Dynamic subcompartmentalization of the mitochondrial inner membrane. *J Cell Biol* 175: 237 – 247

Wasilewski M, Semenzato M, Rafelski SM, Robbins J, Bakardjiev AI, Scorrano L (2012) Optic atrophy 1-dependent mitochondrial remodeling controls steroidogenesis in trophoblasts. *Curr Biol* 22: 1228 – 1234

Wittig I, Braun HP, Schagger H (2006) Blue native PAGE. *Nat Protoc* 1: 418 – 428

Wittig I, Schagger H (2009) Supramolecular organization of ATP synthase and respiratory chain in mitochondrial membranes. *Biochim Biophys Acta* 1787: 672 – 680

Wurm CA, Jakobs S (2006) Differential protein distributions define two sub-compartments of the mitochondrial inner membrane in yeast. *FEBS Lett* 580: 5628 – 5634

Yamaguchi R, Lartigue L, Perkins G, Scott RT, Dixit A, Kushnareva Y, Kuwana T, Ellisman MH, Newmeyer DD (2008) Opa1-mediated cristae opening is Bax/Bak and BH3 dependent, required for apoptosis, and independent of Bak oligomerization. *Mol Cell* 31: 557 – 569

Zuchner S, Mersiyanova IV, Muglia M, Bissar-Tadmouri N, Rochelle J, Dadali EL, Zappia M, Nelis E, Patitucci A, Senderek J, Parman Y, Evgrafov O, Jonghe PD, Takahashi Y, Tsuji S, Pericak-Vance MA, Quattrone A, Battaloglu E, Polyakov AV, Timmerman V *et al* (2004) Mutations in the mitochondrial GTPase mitofusin 2 cause Charcot-Marie-Tooth neuropathy type 2A. *Nat Genet* 36: 449 – 451